

Efficient stabilization of zero-slope walking for bipedal robots following their passive fixed-point trajectories

Aikaterini Smyrli, Georgios A. Bertos, *Member, IEEE*, and
Evangelos Papadopoulos, *Senior Member, IEEE*

Abstract— This paper presents an efficient method of stabilizing the gait of an underactuated biped with compliant legs and semicircular feet. First, the model is defined, incorporating elements that are often present in experimental biped robots. The biped's passive behavior is studied through numerical simulations that provide insight into the gravity's contribution as an energy input to the system. Based on this study, it is shown that an augmented biped -with the addition of a counterweight joint at the hip- is able to perform stable gaits with minimal input. This design is implemented easily as it does not require ankle torques; instead, both motors are mounted at the biped's hip. The control law used for the stabilization is the combination of virtual-gravity components with non-linear PD terms. The stable gaits performed by the augmented biped on level floor strongly resemble the passive gaits of the original biped walking on a slope, resulting in an efficient, natural-like motion of low transport cost.

I. INTRODUCTION

Through the study of human gait mechanics, a special class of passive bipedal machines has emerged, which exhibit walking on negative slopes as a natural passive-dynamic mode [1]. Several robot designs take advantage of this behavior, relying on their passive dynamics and only using actuators as the means of compensating energy losses [2][3][4][5][6]. This approach results in efficient forms of transport, as the required energy input is minimal.

Most of the published research on the dynamics of bipedal machines have made the assumption of rigid feet and thus fail to simulate the energetic losses of damped deformations, as well as the dynamics during the double stance phase of walking. Energetic losses in such models are only present due to the velocity discontinuity just-before and just-after instantaneous impacts, which are computed via the conservation of angular momentum [2]. Works that have employed models with compliance have neglected damping in leg axial impedance [7][8]. However, leg impedance has been proven to be an important factor that needs to be considered in studying bipedal walking [9][10].

Virtual gravity control has been proposed as a method of replicating passive gaits on level ground with minimal torque input. In an effort to provide each of the two legs with its proper input torque, most of this type of research concerns actuated robots with active ankle joints [2][4]. Such an approach is in practice difficult to embody in a biped robot, as one end of the ankle actuator must be fixed to the ground.

To bypass this limitation, control schemes have been proposed that result in stable biped gaits using a single actuator for the inter-leg angle [11][12][13]. As a

consequence of applying the same torque magnitude on both limbs, these schemes fail to replicate the biped's optimal passive motion on level floor.

Other studies have incorporated a torso for housing the two leg actuators, thus mimicking the human anatomy. The torso's position was mechanically constrained through the use of an angle-bisecting mechanism [14], and a PD controller was used to keep the torso up [15]. Virtual gravity control laws were used for a biped with a torso, which is kept in position by a linear PD controller located at the hip [16]. However, the authors consider a fully actuated model and include actuated ankle joints, bypassing the problem of underactuation, and resulting in the limitations mentioned above [16]. Also, the use of linear PD terms overwrites the natural dynamics of the biped, as they intervene in the dynamics considerably, even for small torso deviations.

In this paper, a passive biped initial model is studied that includes elastic and damping elements, providing a more accurate description of the energy lost during a stride, and allowing for detailed simulation of the heelstrike collision and for analysis of the gradual support transfer between the two compliant legs. This model also includes point masses at the hip and the feet of the biped; these are semicircular in shape, acting as a partial substitute of ankle joints [11]. The point masses attached to the feet are equally important, as they allow the dynamic study of their pendulum-like motion during the swing phase.

It is shown that instead of an upward torso, augmenting the biped with a hip counterweight results in repetitive gaits under a virtual gravity controller, by optimally using the counterweight's contribution to the biped's underactuated dynamics. The actuated DOFs are the angles between each of the two legs and the hip counterweight. However, the gaits performed with this controller are found to be non-stabilizable by design. A stabilizing controller that includes both a model-based virtual gravity part and non-linear PD terms is developed, partially compensating the gravitational input absent in level ground locomotion. Strategic selection of the nonlinear PD controller's gains efficiently stabilizes the closed-loop system, while the gaits performed remain almost identical to the ones performed by the passive model.

This paper is organized in six sections. Section II presents the derivation of the initial passive biped model. In Section III, the model is studied for various parameter combinations and an optimal parameter set is selected as the nominal one. In Section IV, an augmented underactuated virtual gravity biped model is developed as to better take advantage of its passive dynamics. A stabilizing controller that includes both virtual gravity and non-linear PD terms is studied and tested in Section V, where our study's results are also presented. In Section VI conclusions are drawn.

The authors are with the School of Mechanical Engineering, National Technical University of Athens, (e-mail: egpapado@central.ntua.gr, tel: +30 210-772-1440).

II. PASSIVE BIPED MODELING

The model studied initially in this paper differs from what has been published to date, in that it incorporates elastic and damping elements resulting in *compliant* legs. Following published results [11], semicircular profiles have been chosen for the model's feet, in order to facilitate step-to-step transitions and help propel the biped forward, imitating the existence of an active ankle joint. The model also includes three point-masses, one of which is located at the hip while the remaining two correspond to the two feet.

The biped model is presented in Fig. 1 during the single stance phase of walking, where only one of the two legs is in contact with the ground. The parameters that define the passive model are the uncompressed leg length, L_{nat} , the hip point mass M , the foot point mass m , the foot radius r , the foot mass distance l , the spring constant k and the damping constant b . The biped walks passively on a floor of slope α , here $\alpha < 0$. The system is described by the generalized vector \mathbf{q} , which consists of the stance leg angle θ , the stance leg length L_1 , the swing leg angle ψ , and the swing leg length L_2 :

$$\mathbf{q} = [\theta, L_1, \psi, L_2]^T \quad (1)$$

The assumptions made in this work are as follows: (i) the floor and feet are considered to be inelastic and non-compliant, (ii) the feet in contact with the ground perform rolling without slipping, (iii) floor contact of the swing foot during its forward advancement in the single stance phase is ignored (iv) there is no distinction between left and right leg, and (v) leg angles θ and ψ are defined in opposing directions.

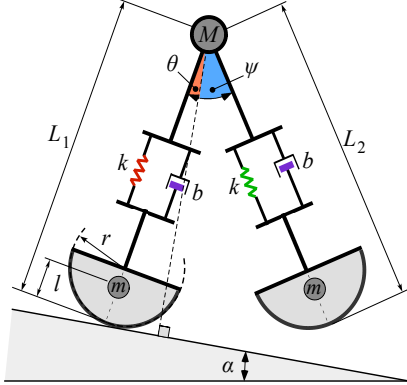


Figure 1. Passive biped model during the single stance phase of walking.

A. Single stance phase

During the single stance phase, the system is described by \mathbf{q} given in (1), also see Fig. 1. The corresponding equations of motion are written in the Euler-Lagrange formulation as:

$$\mathbf{M}(\mathbf{q})\ddot{\mathbf{q}} + \mathbf{C}(\mathbf{q}, \dot{\mathbf{q}})\dot{\mathbf{q}} + \mathbf{K}(\mathbf{q}) + \mathbf{G}(\mathbf{q}) = \mathbf{0} \quad (2)$$

where \mathbf{M} is a 4x4 inertia matrix, \mathbf{C} is a 4x4 matrix that contains centrifugal, Coriolis and damping terms, \mathbf{K} is the 4x1 stiffness vector and \mathbf{G} is a 4x1 vector containing gravitational terms. The details of these elements have been spared here due to space limitations.

B. Double stance phase

As Fig. 2 shows, during the double stance phase only two variables are independent; the other variables are subject to geometric limitations that result from assumptions (i) and (ii). These translate to a set of two constraints that must remain true during the time both legs are in contact with the ground:

$$s_1(\mathbf{q}) = (L_1 - r)\cos\theta - (L_2 - r)\cos\psi = 0 \quad (3)$$

$$s_2(\mathbf{q}) = d_{HS} - d + r(\theta_{HS} - \theta + \psi_{HS} - \psi) = 0 \quad (4)$$

where d is the distance of the two semicircular feet centers:

$$d = (L_1 - r)\sin\theta + (L_2 - r)\sin\psi \quad (5)$$

and the subscript *HS* denotes the variables' values at Heel-Strike (HS), see Fig. 2.

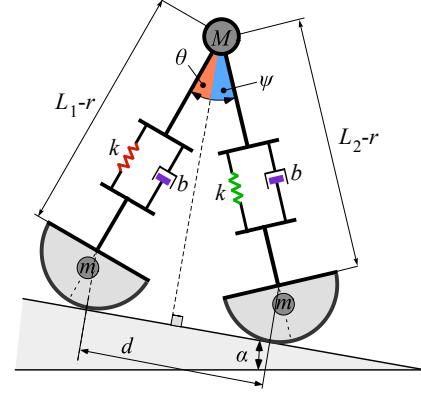


Figure 2. Passive biped model during the double stance phase of walking.

In order for conditions (3) and (4) to be satisfied, the dynamic equations must be modified with the addition of generalized constraint forces:

$$\mathbf{f}_{constr.} = \mathbf{\Pi}^T(\mathbf{q})\boldsymbol{\lambda} \quad (6)$$

In (6), $\boldsymbol{\lambda}$ is the vector containing the Lagrange multipliers λ_1 and λ_2 , corresponding to constraints s_1 and s_2 respectively. The 4x2 constraint matrix $\mathbf{\Pi}$ is derived according to Lagrange's formulation:

$$\pi_{jk} = \frac{\partial s_j}{\partial q_k}, \quad j=1\dots 2, k=1\dots 4 \quad (7)$$

Then, the dynamic equations of the double stance phase can be expressed as:

$$\begin{aligned} \mathbf{M}(\mathbf{q})\ddot{\mathbf{q}} + \mathbf{C}(\mathbf{q}, \dot{\mathbf{q}})\dot{\mathbf{q}} + \mathbf{K}(\mathbf{q}) + \mathbf{G}(\mathbf{q}) - \mathbf{\Pi}^T(\mathbf{q})\boldsymbol{\lambda} &= \mathbf{0} \\ s_1(\mathbf{q}) &= 0 \\ s_2(\mathbf{q}) &= 0 \end{aligned} \quad (8)$$

where the rest of the matrices are as defined earlier.

C. Phase transitions

Having defined the two phases of a full step, two conditions need to be derived upon which the phase transitions occur. The first is the event HS, which marks the end of the single stance phase and is composed of three separate conditions that need to be satisfied at the same time. These are the foot-on-ground condition, the swing leg advancement condition, and the swing leg retraction condition, defined respectively by (9)-(11):

$$(L_1 - r)\cos\theta - (L_2 - r)\cos\psi = 0 \quad (9)$$

$$\psi > 0 \quad (10)$$

$$\frac{d}{dt}[(L_1 - r)\cos\theta - (L_2 - r)\cos\psi] < 0 \quad (11)$$

The second event is the Toe-Off (TO), which ends the double stance phase and occurs when the spring force overcomes the gravity force projected on the leg:

$$k(L_1 - L_{nat}) - mg\cos(\alpha - \theta) > 0 \quad (12)$$

D. Step function

We first define the system's state vector \mathbf{x} , which is composed of the generalized variables \mathbf{q} and velocities $\dot{\mathbf{q}}$:

$$\mathbf{x} = [\theta, \dot{\theta}, L_1, \dot{L}_1, \psi, \dot{\psi}, L_2, \dot{L}_2]^T \quad (13)$$

Let the state vector be \mathbf{x}_n at the beginning of the n^{th} step. The step begins with the single stance phase, which assumes \mathbf{x}_n as its initial condition, advances the model's state in the way described by (2) and ends at HS, with an updated state vector $\mathbf{x}_{n,\text{HS}}$. This process may be written in the form of a discrete function, f_1 , for the single stance phase:

$$\mathbf{x}_{n,\text{HS}} = f_1(\mathbf{x}_n) \quad (14)$$

After the HS, the double stance phase (8) starts with initial condition $\mathbf{x}_{n,\text{HS}}$ and ends at TO, with a final state vector $\mathbf{x}_{n,\text{TO}}$. The discrete function describing this transition is f_2 :

$$\mathbf{x}_{n,\text{TO}} = f_2(\mathbf{x}_{n,\text{HS}}) = f_2(f_1(\mathbf{x}_n)) \quad (15)$$

As a result of assumptions (iv) and (v), the state variables must be transformed before the beginning of the $(n+1)^{\text{th}}$ step:

$$\begin{aligned} \theta_{n+1} &= -\psi_{n,\text{TO}}, \quad \psi_{n+1} = -\theta_{n,\text{TO}} \\ \dot{\theta}_{n+1} &= -\dot{\psi}_{n,\text{TO}}, \quad \dot{\psi}_{n+1} = -\dot{\theta}_{n,\text{TO}} \\ L_{1,n+1} &= L_{2,n,\text{TO}}, \quad L_{2,n+1} = L_{1,n,\text{TO}} \\ \dot{L}_{1,n+1} &= \dot{L}_{2,n,\text{TO}}, \quad \dot{L}_{2,n+1} = \dot{L}_{1,n,\text{TO}} \end{aligned} \quad (16)$$

This is achieved by multiplying the state vector $\mathbf{x}_{n,\text{TO}}$ with the 8×8 symmetric matrix \mathbf{T} , resulting in the initial state \mathbf{x}_{n+1} :

$$\mathbf{x}_{n+1} = \mathbf{T}\mathbf{x}_{n,\text{TO}} \quad (17)$$

The *non-zero* elements of \mathbf{T} result from (16) as: $t_{15}=t_{26}=t_{51}=t_{62}=-1$, $t_{37}=t_{48}=t_{73}=t_{84}=1$. Finally, we can define a discrete function that describes the transition from \mathbf{x}_n to \mathbf{x}_{n+1} . We call this *step function* \mathbf{P} :

$$\mathbf{x}_{n+1} = \mathbf{T}f_2(f_1(\mathbf{x}_n)) \triangleq \mathbf{P}(\mathbf{x}_n) \quad (18)$$

E. Fixed points

Fixed points of the system are state vectors \mathbf{x}^* for which the step function output \mathbf{x}_{n+1} coincides with its input \mathbf{x}_n :

$$\mathbf{x}^* = \mathbf{P}(\mathbf{x}^*) \quad (19)$$

To locate these points, a Newton-Raphson numerical method is employed:

$$\mathbf{x}_n^{(k+1)} = \mathbf{x}_n^{(k)} + (\mathbf{I}_{8 \times 8} - \nabla \mathbf{P}(\mathbf{x}_n^{(k)}))^{-1} [\mathbf{P}(\mathbf{x}_n^{(k)}) - \mathbf{x}_n^{(k)}] \quad (20)$$

Eq. (20) is repeatedly solved until numerical convergence, according to the following empirical criterion:

$$\left\| \mathbf{x}_n^{<k+1>} - \mathbf{x}_n^{<k>} \right\|_{\infty} < 10^{-6} \quad (21)$$

Fixed points found in this way constitute repetitive gaits performed by the biped.

F. Fixed point stability

Fixed points of dynamical systems can be characterized regarding their stability. This is possible through the local linearization of function \mathbf{P} around the fixed point, \mathbf{x}^* :

$$\Delta \mathbf{x}_{n+1}^* = \left. \frac{\partial \mathbf{P}(\mathbf{x}^*)}{\partial \mathbf{x}} \right|_{\mathbf{x}=\mathbf{x}^*} \Delta \mathbf{x}_n^* \triangleq \mathbf{A} \Delta \mathbf{x}_n^* \quad (22)$$

where $\Delta \mathbf{x} = \mathbf{x} - \mathbf{x}^*$, is a small deviation of the state vector from its fixed-point value.

The stability of the discrete system defined by \mathbf{P} at the fixed point \mathbf{x}^* is characterized by the eigenvalues of matrix \mathbf{A} : all eigenvalues of \mathbf{A} must have a magnitude less than 1 in order for the fixed point to be stable.

III. PASSIVE GAIT ON SLOPE

The biped's passive dynamics are described by (18). Through dimensional analysis of \mathbf{P} , it is shown that system dynamics depend only on a set of six non-dimensional parameters: slope angle α , damping parameter β , elasticity parameter κ , hip-to-foot mass ratio μ , foot mass distribution parameter λ and rolling factor ρ . These are defined in Table I.

Eq. (20) is employed to locate fixed points of systems with varying non-dimensional parameter combinations. Once a fixed point is found, its stability is evaluated by studying the eigenvalues of the linearized matrix \mathbf{A} in (22).

Fig. 3 presents the magnitude of the maximum eigenvalue of gaits resulting from systems of various parameter combinations. Gaits corresponding to points plotted in green are stable, while red points indicate unstable gaits. Nominal parameter values were selected through a minmax algorithm applied to the eigenvalues of \mathbf{A} and are listed in Table I. These constitute an optimal system, in the sense of passive stability. Each of the plots in Fig. 3 corresponds to variations of one of the system-defining parameters, while the rest of the parameters remain fixed at their nominal values.

Fig. 4 presents the leg-angle passive gait phase space of the system composed by non-dimensional parameters at their *nominal* values given in Table I.

TABLE I. NON-DIMENSIONAL MODEL PARAMETERS.

Parameter	Value	Nominal Value
α	α	-2°
β	$b\sqrt{L_{nat}}/(M\sqrt{g})$	3.63
κ	$kL_{nat}/(Mg)$	29.7
λ	l/L_{nat}	0.14
μ	m/M	0.016
ρ	r/L_{nat}	0.363

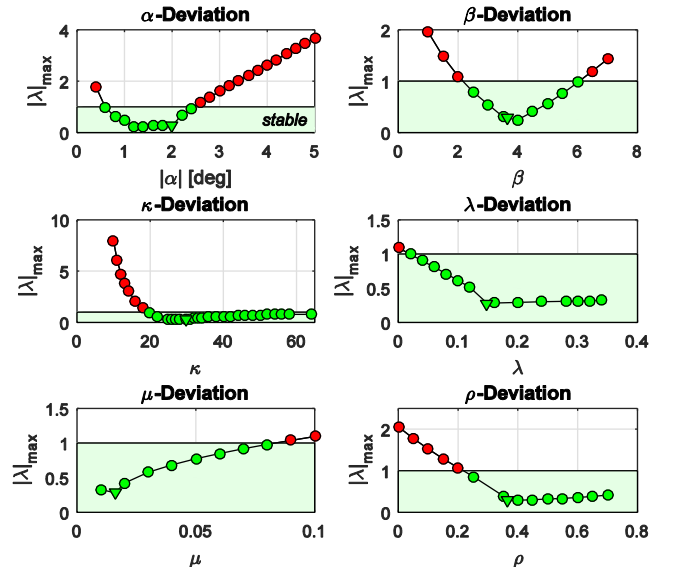


Figure 3. Stability analysis of parameter variations.

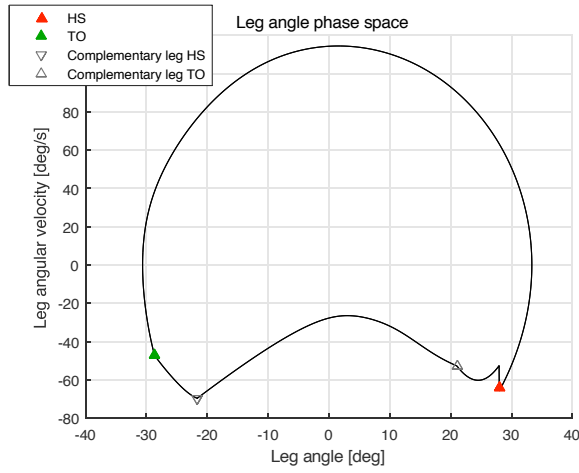


Figure 4. Leg-angle passive dynamics stable phase space, nominal system.

IV. LEVEL GROUND WALKING

The passive gaits achieved require a slope $\alpha < 0$. However, if $\alpha = 0$, the slope terms \mathbf{G}_α driving walking disappear and passive walking is not achieved. Therefore, we explore the idea of substituting these terms with actuation, when $\alpha = 0$.

A. Gravity compensation terms

The virtual gravity control approach suggests that in order for the biped on level ground to act as if it walked passively on slope α , the theoretical actuation input $\mathbf{f}_{g,th}$ must be:

$$\mathbf{f}_{g,th} = [f_\theta, f_{L_1}, f_\psi, f_{L_2}]^T = \mathbf{G}_0(\mathbf{q}) - \mathbf{G}_\alpha(\mathbf{q}) \quad (23)$$

where \mathbf{G}_α is the gravity vector in (2) and is given by (24), and $\mathbf{G}_0 = \mathbf{G}_\alpha$ with $\alpha = 0$. The elements of \mathbf{G}_α are as follows:

$$\begin{aligned} g_1 &= g\{ (M+m)[r \sin a + (L_1 - r) \sin(a - \theta)] \\ &\quad + m[r \sin a + (l - r) \sin(a - \theta)] \} \\ g_2 &= g(M+m) \cos(a - \theta) \\ g_3 &= gm(L_2 - l) \sin(a + \psi) \\ g_4 &= -gm \cos(a + \psi) \end{aligned} \quad (24)$$

Our model contains four degrees of freedom, of which two need to be controlled: these are the leg angles θ and ψ . Leg lengths L_1 and L_2 are not to be controlled since the implementation of axial actuators in a biped robot would present design difficulties and increase power consumption; the corresponding terms, f_{L_1} and f_{L_2} , have been spared here.

The terms of (23) corresponding to the angular degrees of freedom θ and ψ , i.e., f_θ and f_ψ , were computed during a step of the nominal biped (Table I) and are plotted in Fig. 5.

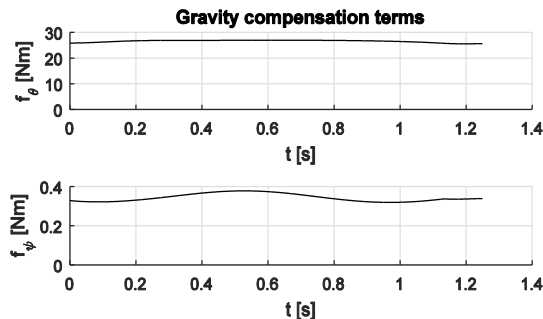


Figure 5. Gravity compensation input torques.

It is observed that f_θ and f_ψ have an almost flat profile. However, they are of significantly different magnitude, which highlights the need for using two separate actuators to control the biped.

B. Augmented model

Observation of Fig. 5 leads to the conclusion that each of the two leg actuators can be mounted between their corresponding leg and a third link, resulting in the augmented biped model shown in Fig. 6.

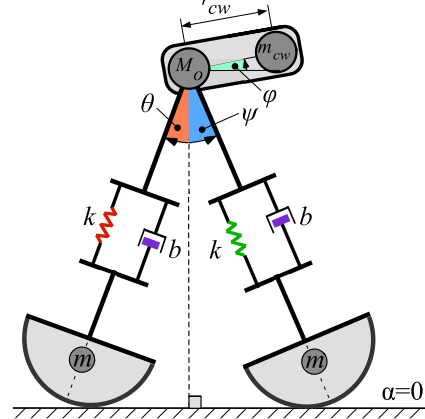


Figure 6. The augmented biped model for level ground walking.

The augmented model's generalized vector during single stance phase, \mathbf{q}^+ , includes the third link's angle ϕ , in addition to the rest of the previously used generalized variables:

$$\mathbf{q}^+ = [\theta, L_1, \psi, L_2, \phi]^T \quad (25)$$

We select actuator torques to be:

$$\mathbf{u}_g = \begin{bmatrix} u_{g1} \\ u_{g2} \end{bmatrix} = \begin{bmatrix} f_\theta \\ f_\psi \end{bmatrix} \quad (26)$$

Therefore, the input to the augmented model becomes:

$$\mathbf{f} = \mathbf{S} \mathbf{u}_g = \begin{bmatrix} 1 & 0 \\ 0 & 0 \\ 0 & 1 \\ 0 & 0 \\ 1 & -1 \end{bmatrix} \begin{bmatrix} f_\theta \\ f_\psi \end{bmatrix} = \begin{bmatrix} f_\theta \\ 0 \\ f_\psi \\ 0 \\ f_\theta - f_\psi \end{bmatrix} \quad (27)$$

and satisfies (23) partially, by providing leg angles θ and ψ with the exact torques needed to replicate their passive trajectories. Note that this control scheme does not intend to keep the newly introduced link in a vertical, torso-like position; instead it is used as a mounting device for the two leg motors. As such, it is subject to the almost constant motor reaction torque sum:

$$T_{hip} = f_\theta - f_\psi \quad (28)$$

By selecting this link to have its center of mass located at a distance r_{cw} from the biped's hip joint, gravitational torque is developed:

$$T_{cw} = m_{cw} r_{cw} \cos \phi \quad (29)$$

where m_{cw} is the link's mass and ϕ is the link's angle with respect to the horizontal axis. Then, this link acts as a counterweight by balancing the motor reaction torque if the following relation holds:

$$T_{cw} = T_{hip} \quad (30)$$

In practice neither T_{hip} nor T_{cw} remain constant throughout a step: the former depends on the gravity compensation terms of Fig. 5, while the latter depends on the counterweight angle φ . The mean value of the counterweight angle φ must be close to zero in order for the link to optimally act as a counterweight. Assuming that this is the case, (28) and (29) are combined to define a design relationship for $m_{cw}r_{cw}$:

$$m_{cw}r_{cw} = \max(T_{hip}) \quad (31)$$

To better replicate the passive model's dynamic behavior, the augmented model's hip mass was given a value of M_0 so that the total mass supported by the legs is still M :

$$M = M_0 + m_{cw} \quad (32)$$

Finally, to obtain level ground walking, the slope angle α was set to zero. The rest of the augmented model's parameters exist in the passive model as well, and their values are kept unchanged.

The step function \mathbf{P} of the augmented model was described analytically, and its fixed points were located and evaluated. Simulations showed that the augmented biped manages to capture the dynamic trajectories of the passive biped with low energetic cost, but its fixed points were not stabilizable by any combination of m_{cw} and r_{cw} , resulting in the biped "falling down" after about 500 steps.

V. LEVEL GROUND GAIT STABILIZATION

Gait stabilization is very important for legged robots, as they are often used on rough or irregular terrain. Moreover, encoder feedback errors introduce some level of disturbance to the system. For these reasons, the biped robot's controller must guarantee its orbital gait stability.

A. Control scheme

To stabilize the system, the motor control torque applied between the stance leg and the counterweight link was enhanced with two additional third-order nonlinear PD terms:

$$\mathbf{u} = \mathbf{u}_g + \mathbf{u}_{PD} = \mathbf{u}_g + \begin{bmatrix} -K_p(\varphi - \varphi_d)^3 - K_d(\dot{\varphi} - \dot{\varphi}_d)^3 \\ 0 \end{bmatrix} \quad (33)$$

The subscript "d" in (33) stands for counterweight desired values. These are obtained by simulations ran with the virtual gravity input only, as discussed previously.

The choice of raising φ errors to the third power was made in order for the PD part of the controller to compensate only when these errors become significant; this also allows choosing relatively small gains. However, aside from stabilization, an important reason for this controller is that the biped natural dynamics are not overwritten when the biped moves within its fixed-point orbit, as would result if linear terms were used, i.e. proportional to the φ error.

Picking gains K_p and K_d with trial and error is relatively easy; choosing them more systematically is discussed next. Simulations of the augmented biped model for different combinations of these gains were conducted and resulting gaits were evaluated in terms of stability, energetic cost of transport, resemblance to the passive trajectories and maximum motor input torque, as discussed next.

B. Results

As mentioned above, the control scheme PD terms (33) were introduced to achieve stable gaits on level floor.

Stability of the augmented biped model on level ground is investigated in Fig. 7a with respect to the PD controller gains. As expected, the gait performed for a gain combination $(K_p, K_d)=(0,0)$ is unstable. This gain selection corresponds to the virtual gravity control scheme given by (26). Another region of instability results for low K_p and high K_d , shown as a yellow region in in Fig. 7a. However, it is observed that many other gain combinations lead to stable gaits. This is especially useful in designing a stabilizing controller for the biped on level ground, as it allows us to ensure stability of the system, while simultaneously satisfying additional criteria.

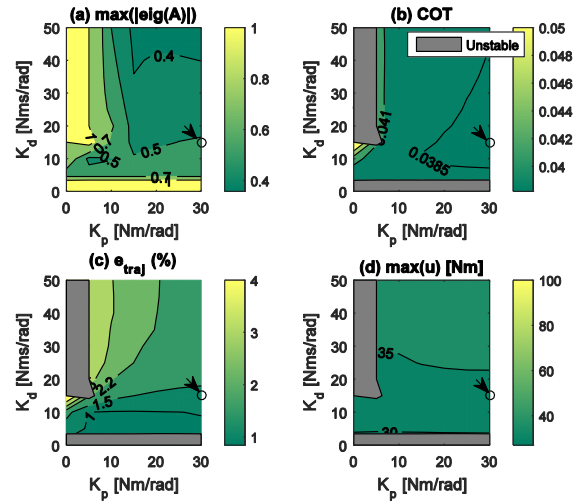


Figure 7. Augmented biped model gait characteristics for combinations of (K_p, K_d) : (a) Stability. (b) COT. (c) Trajectory error. (d) Max. motor torque.

Second to stability, an important factor that needs to be optimized is the achieved gaits' energetic efficiency. This is usually quantified in the form of COT (cost of transport):

$$COT = \frac{E_{in}}{(M + 2m)g\Delta x} \quad (34)$$

where E_{in} is the total energy input, supplied by the robot's actuators and calculated by the time integral of absolute power, as it is assumed that the motor drives are not capable of energy regeneration during braking, while Δx is the distance travelled. It has been shown that for bipeds walking passively on a slope of α (by extension, imitating passive walk of slope α), the COT is equal to $\tan\alpha$ [7]. This calculates to an optimal value of 0.035 for the nominal slope angle.

Fig. 7b presents the COT of the gaits performed by the augmented biped model under control scheme (33). Computed COT values are comparable to the optimal one, but slightly greater. This is partly accounted for by the non-regenerative limitation of the drives, while the use of the PD controller also results to greater power consumption. However, the closeness of the obtained values to the optimal COT suggests that despite active control, the actuated biped moves almost as efficiently as the passive one.

Achieved gaits were also evaluated regarding their resemblance to the passive biped's gait. This was quantified through trajectory deviations, by adding the mean relative trajectory errors of the four generalized variables present in both the augmented and the passive model and their velocities, for a total simulation time of $\Delta T = t_{\text{max}} - t_{\text{min}}$:

$$e_{traj} = \sum_{q_i=1}^4 \left\{ \frac{1}{\Delta T} \int_{t_{min}}^{t_{max}} \frac{|q_i(t) - q_i^+(t)|}{\max(|q_i|_{t=t_{min}}^{t=t_{max}})} dt \right\} + \sum_{\dot{q}_i=1}^4 \left\{ \frac{1}{\Delta T} \int_{t_{min}}^{t_{max}} \frac{|\dot{q}_i(t) - \dot{q}_i^+(t)|}{\max(|\dot{q}_i|_{t=t_{min}}^{t=t_{max}})} dt \right\} \quad (35)$$

Small values of the trajectory error, e_{traj} , correspond to a high degree of resemblance between passive and augmented model gaits. Fig. 7c presents the value of e_{traj} for gaits resulting from various combinations of controller gains. In total, it is shown that the augmented model under the selected control scheme results in satisfactory gait resemblance with respect to the passive gait.

The final subject of investigation was the maximum motor input torque. This was calculated as the maximum value of the input torques (33) during one step, see Fig. 7d.

As an example, we study the gait corresponding to $(K_p, K_d)=(30,15)$, a selection which has been marked with an arrow in Fig. 7. This gain selection results in a stable gait with a maximum eigenvalue magnitude of 0.51, with a *COT* of 0.038, and state vector trajectories almost identical to the passive gait's, with a total error of less than 1.4%, while motor torque requirements remain under 35 Nm, for a total biped weight of 80 kg. Fig. 8 presents the counterweight link's state variations and input torque during five consecutive steps, with initial conditions chosen outside the model's fixed-point trajectory.

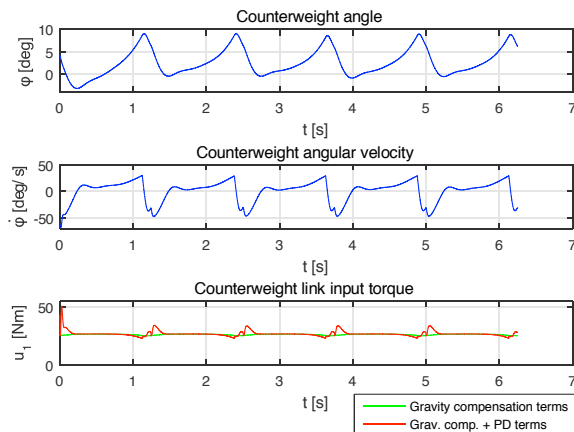


Figure 8. Augmented model gait stabilization for $(K_p, K_d)=(30, 15)$.

It can be seen that the developed controller manages to stabilize the system and guarantee convergence to a stable gait. The PD terms mostly intervene to correct the initial conditions. After this initial correction, they only compensate at the beginning of each step of the stable gait, allowing the expression of the biped's natural dynamics thereafter.

VI. CONCLUSION

A model of a passive biped robot with compliant legs and semicircular feet was developed. Its design was optimized with respect to the stability of its passive gait on inclined terrain. To replicate this gait on level ground, and therefore to supply the robot with the input torques dictated by the virtual gravity methodology, the model was augmented with the

addition of an extra link at the hip joint. To stabilize the biped, this link was given the form of an almost-horizontally positioned counterweight, taking advantage of the input torque profiles. The control law developed for the stabilization of the augmented biped is a combination of virtual-gravity components with non-linear PD terms. The stable gaits performed by the augmented biped on level floor strongly resemble the passive gaits of the original biped walking on a slope, resulting in an efficient, natural-like motion of low transport cost.

Since the swing leg has no mechanism to "clear" the floor, as a knee mechanism would allow, we plan to build a robot with swing leg retraction and operate it under the developed control scheme for validation and optimization.

REFERENCES

- [1] McGeer, T., "Passive Dynamic Walking", *The International Journal of Robotics Research*, 1990, 9(2): pp. 62-82.
- [2] Espiau, B., and Goswami, A., "Compass gait revisited", in *IFAC Proceedings Volumes*, 1994, 27(14): pp. 839-846.
- [3] Spong, M. W. (1999b), "Passivity Based Control of the Compass Gait Biped", *IFAC World Congress*, Beijing, China, B, pp. 19-24, 1999.
- [4] Spong, M. W. and Bhatia, G., "Further results on control of the compass gait biped", *IEEE/RSJ Int. Conf. on Intelligent Robots and Systems (IROS '03)*, Las Vegas, USA, 2003, vol.2, pp.1933-1938.
- [5] Asano, F., Luo, Z.W., and Yamakita, M., "Unification of dynamic gait generation methods via variable virtual gravity and its control performance analysis", *IEEE/RSJ Int. Conf. on Intelligent Robots and Systems (IROS '04)*, Sendai, Japan, 2004, vol.4, pp. 3865-3870.
- [6] Cherouvim, N. and Papadopoulos, E., "Energy Saving Passive-Dynamic Gait for a One-Legged Hopping Robot," *Robotica*, Vol. 24, No. 4, July 2006, pp. 491-498.
- [7] Alexander, R., "A model of bipedal locomotion on compliant legs", *Philosophical Transactions of the Royal Society of London, Series B: Biological Sciences*, 1992, 338(1284): pp. 189-198.
- [8] Godage, I. S., Wang, Y. and Walker, I. D., "Energy based control of compass gait soft limbed bipeds", *IEEE/RSJ Int. Conf. on Intelligent Robots and Systems (IROS '14)*, Chicago, USA, 2014, pp. 4057-4064.
- [9] Bertos, G.A., Childress, D.S., Gard, S.A., "A steady state sinusoidal analysis method to identify the mechanical impedance of the human locomotor system during able-bodied walking", *26th International Conference of Rehabilitation Engineering & Assistive Technology of North America (RESNA '03)*, Atlanta, USA, 2003.
- [10] Bertos G. A., Childress D. S. and Gard S. A., "The vertical mechanical impedance of the locomotor system during human walking with applications in rehabilitation", *IEEE Int. Conf. on Rehabilitation Robotics, (ICORR '05)*, Chicago, USA, 2005, pp. 380-383.
- [11] Asano, F. and Luo, Z.W., "On Energy-Efficient and High-Speed Dynamic Biped Locomotion with Semicircular Feet", *IEEE/RSJ Int. Conf. on Intelligent Robots & Systems (IROS '98)*, Beijing, China, 2006, pp. 5901-5906.
- [12] Tang, J. Z., Boudali, A. M. and Manchester, I. R., "Invariant funnels for underactuated dynamic walking robots: New phase variable and experimental validation", *IEEE International Conference on Robotics and Automation (ICRA '17)*, Singapore, 2017, pp. 3497-3504.
- [13] Xiao, X. Ma, O. and Asano, F., "Control Walking Speed by Approximate-kinetic-model-based Self-adaptive Control on Underactuated Compass-like Bipedal Walker", *IEEE Int. Conf. on Robotics and Automation (ICRA '17)*, Singapore, 2017, pp. 4729-4734.
- [14] Asano, F. and Luo, Z.W., "Pseudo virtual passive dynamic walking and effect of upper body as counterweight", *IEEE/RSJ Int. Conf. on Int. Robots & Systems (IROS '08)*, Nice, France, 2008, pp. 2934-2939.
- [15] Narukawa, T., Takahashi, M. and Yoshida, K., "Biped locomotion on level ground by torso and swing-leg control based on passive-dynamic walking", *IEEE/RSJ International Conference on Intelligent Robots and Systems (IROS '05)*, Edmonton, Canada, 2005, pp.4009-4014.
- [16] Sasaki, H. and Yamakita, M., "Efficient Walking Control of Robot with Torso Based on Passive Dynamic Walking", *IEEE Int. Conf. on Mechatronics (ICM '07)*, Kumamoto, Japan, 2007, pp: 1-5.